Determinants of Ligand Binding to cAMP-Dependent Protein Kinase†

Philippe H. Hünenberger,*,‡ Volkhard Helms,‡ Narendra Narayana,§ Susan S. Taylor,‡ and J. Andrew McCammon‡,||

Department of Chemistry and Biochemistry and Department of Pharmacology, University of California at San Diego, 9500 Gilman Drive, La Jolla, California 92093-0365, and Department of Chemistry and Molecular Biology, University of Chicago, 924 East 57th Street, Chicago, Illinois 60637

Received August 25, 1998; Revised Manuscript Received October 28, 1998

ABSTRACT: Protein kinases are essential for the regulation of cellular growth and metabolism. Since their dysfunction leads to debilitating diseases, they represent key targets for pharmaceutical research. The rational design of kinase inhibitors requires an understanding of the determinants of ligand binding to these proteins. In the present study, a theoretical model based on continuum electrostatics and a surface-area-dependent nonpolar term is used to calculate binding affinities of balanol derivatives, H-series inhibitors, and ATP analogues toward the catalytic subunit of cAMP-dependent protein kinase (cAPK or protein kinase A). The calculations reproduce most of the experimental trends and provide insight into the driving forces responsible for binding. Nonpolar interactions are found to govern protein−ligand affinity. Hydrogen bonds represent a negligible contribution, because hydrogen bond formation in the complex requires the desolvation of the interacting partners. However, the binding affinity is decreased if hydrogen-bonding groups of the ligand remain unsatisfied in the complex. The disposition of hydrogen-bonding groups in the ligand is therefore crucial for binding specificity. These observations should be valuable guides in the design of potent and specific kinase inhibitors.

Reversible protein phosphorylation is essential for signal transduction and cellular regulation in eukaryotic cells (*1*). Protein kinases catalyze these reactions and form a superfamily of several hundred known proteins (*2*, *3*). Although these enzymes differ in size, substrate specificity, and mechanism of activation, they all share a homologous catalytic core which comprises nine invariant amino acids and many other highly conserved residues (*3*). cAMP[1]-dependent protein kinase (cAPK or protein kinase A) is involved in the regulation of glycogen metabolism (*4*), gene transcription (*5*, *6*), and in the cell cycle control (*7*, *8*), and is the most fully characterized member of this family (*1*). Since the unregulated activation of protein kinases is implicated in numerous diseases such as cancer (*9*−*11*), small molecules that can potently and selectively inhibit them are of considerable interest as potential drugs (*12*−*17*). In addition, they are extremely valuable tools for clarifying the in vitro and in vivo functions of protein kinases and analyzing complex signal transduction pathways.

The catalytic (C) subunit of cAPK and the isozymes of protein kinase C (PKC) are potently inhibited by the fungal metabolite balanol (Figure 1a, $K_i \approx 4-50$ nM), as well as a number of synthetic derivatives (*12*−*15*). Other protein kinase inhibitors include the isoquinolinesulfonamide derivatives H7, H8, and H89 (*16*, *17*) (Figure 1, panels b−d). H7 and H8 are potent inhibitors of cAPK, cGMP-dependent protein kinases, and PKC. H89 displays the highest affinity and specificity for cAPK ($K_i = 48$ nM). In contrast, ATP binds with a low affinity ($K_d = 10-20$ μM) to the free C subunit of cAPK (*18*−*20*). When the C subunit is complexed with either the regulatory (R) subunit or the inhibitor peptide PKI (*21*), the affinity of the complex toward ATP is higher by a factor 100−1000 (*18*, *22*, *23*). These binding studies reveal that essentially nonpolar inhibitors, such as H89, bind to the C subunit with an affinity comparable to that of ligands which form an extensive network of polar contacts with the enzyme, such as balanol and ATP. They also show that selective removal of individual hydroxyl groups from balanol does not significantly affect the affinity of the inhibitor for cAPK (*14*, *15*), even though these groups are involved in protein−ligand hydrogen bonds (*24*). These observations suggest that polar contacts are not a determinant for high affinity, a finding that is surprising at first sight but can be rationalized by the theoretical model presented here.

A number of crystallographic structures of the C subunit are available, in the form of binary C:L (*24*, *25*), C:I (*26*−*29*), or ternary C:I:L (*27*−*33*) complexes, where L denotes a ligand (inhibitor or ATP mimetic) and I denotes PKI(5−24), an inhibitor peptide derived from PKI (*21*). A low-

† Supported by the NIH Grants GM31749 and GM56553 and the NSF Supercomputer Centers NRAC Grant MCA93S013. P.H.H. acknowledges support from the Swiss National Fund and the Human Frontier Science Program Organization. V.H. is a fellow of the PMMB and LJIS programs and is also supported by a postdoctoral fellowship from DAAD.

* To whom correspondence should be addressed. Phone: (619) 822-1469. Fax: (619) 534-7042. E-mail: phunenbe@ucsd.edu.

‡ Department of Chemistry and Biochemistry.

§ Department of Chemistry and Molecular Biology.

|| Department of Pharmacology.

[1] Abbreviations: cAMP, adenosine 3′,5′-monophosphate; cGMP, guanosine 3′,5′-monophosphate; cAPK, cAMP-dependent protein kinase or protein kinase A; C, catalytic subunit of cAPK; R, regulatory subunit of cAPK; PKI, protein kinase inhibitor; PKC, Ca^{2+}-phospholipid-dependent protein kinase or protein kinase C; H7, 1-(5-isoquinolinesulfonyl)-2-methylpiperazine; H8, *N*-[2-(methylamino)ethyl]-5-isoquinolinesulfonamide; H89, N-[2-(*p*-bromocinnamylamino)ethyl]-5-isoquinolinesulfonamide; ATP, adenosine 5′-triphosphate; GTP, guanosine 5′-triphosphate; ITP, inosine 5′-triphosphate.

10.1021/bi982064g CCC: $18.00
Published on Web 02/03/1999

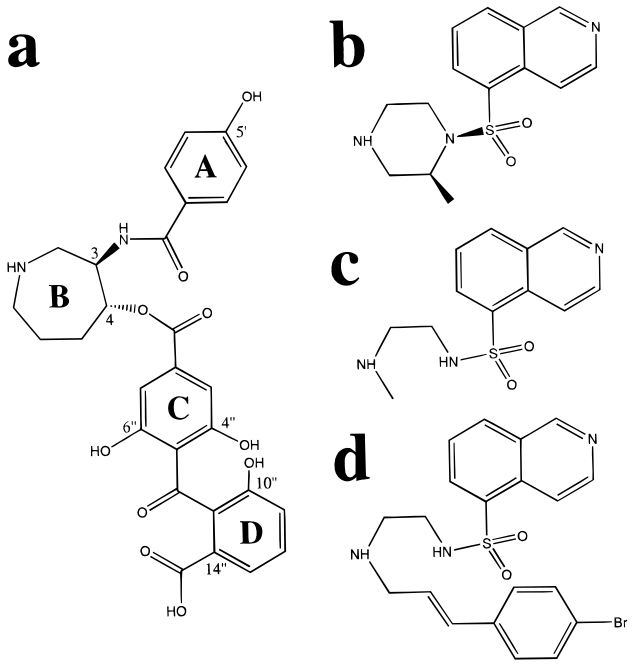

FIGURE 1: Protein kinase inhibitors; (a) (3*R*,4*R*)-balanol or (−)-balanol, the 4″-hydroxyl group is arbitrarily defined as the hydroxyl on ring C closest to the 10″-hydroxyl group in the crystal structure of the cAPK complex (*24*); (b) 1-(5-isoquinolinesulfonyl)-2-methylpiperazine (H7); (c) *N*-[2-(methylamino)ethyl]-5-isoquinolinesulfonamide (H8); (d) *N*-[2-(*p*-bromocinnamylamino)ethyl]-5-isoquinolinesulfonamide (H89); neutral forms are represented, but ionized forms were used in the calculations; the molecules are displayed so as to outline structural analogies.

resolution structure of the apoprotein has also been reported (*28*, *29*, *34*). The C subunit consists of a large, predominantly α-helical lobe, and a small β-sheet-rich lobe, connected by a short linker segment (residues 121−127). In the different crystal structures, the C subunit is found in different conformations resulting from a relative rotation of the two lobes, coupled with concerted motions of peptide segments in the small lobe (*24*, *25*, *28*, *29*, *35*, *36*).

The modes of binding of the different ligands considered here are illustrated in Figure 2. ATP (Figure 2e) binds within the active-site cleft formed by the two lobes. The small lobe and linker segment anchor the nucleotide and stabilize the nontransferable phosphates through hydrogen bonds with backbone amides in the glycine-rich loop (residues 49−57) (*37*) and an ion pair with Lys72 (in turn ion paired with Glu91). The adenine ring is sterically constrained in a hydrophobic pocket and forms three hydrogen bonds with the protein, two of which with the backbone amides of Glu121 and Val123 in the linker segment, and one with Thr183. The large lobe binds the substrate peptide, both magnesium ions via Asp184 and Asn171, and the γ-phosphate.

Balanol and the H-series inhibitors bind within the ATP binding site (*24*, *30*) and act in competition with ATP (*14*, *16*, *17*). Structural details of balanol binding are discussed in an accompanying report (*24*). Balanol (Figure 2a) fits tightly within the active-site cavity. The phenol ring A (Figure 1a) and the benzophenone moiety (rings C and D) of this compound mimic the adenine ring and the triphosphate group of ATP, respectively. Balanol forms a number of hydrogen bonds with the protein, which we briefly summarize here.[2] The 5′-hydroxyl group of ring A forms two hydrogen bonds with the backbone atoms Glu121(O_{CO}) and Val123(H_{NH}) in the linker segment. The carbonyl oxygen atoms of the amide and ester linkages form hydrogen bonds with the side-chain hydroxyl of Thr183 and with the backbone amide of Val57, respectively. The 4″-hydroxyl group of ring C hydrogen bonds with side-chain atoms of Asp184 and Lys72, and the 6″-hydroxyl group with the backbone amides of Gly52, Phe54, and Gly55 in the gylcine-rich loop. The ketone oxygen atom of the benzophenone moiety hydrogen bonds with Phe54(H_{NH}). Finally, the 10″-hydroxyl group of ring D hydrogen bonds with side-chain atoms of Lys72 and Glu91, and the 14″-carboxylate with Ser53(H_{NH} and H_{γ}).

The isoquinoline ring of H-series inhibitors (Figure 2, panels b−d) also mimics the adenine ring of ATP, forming a single hydrogen bond with Val123(H_{NH}) (*30*). In contrast to balanol and Mg_2ATP, H-series inhibitors form fewer polar contacts with the protein. The sulfonamide group of these inhibitors interacts with water molecules in the crystal structure of the complex, yet forms no hydrogen bonds with the protein other than a weak one with Gly50(H_{NH}) in the case of H8 and H89. Superimpositions of the crystal structures of cAPK complexes involving H7, H8, H89, and balanol place the positive ammonium group in a similar protein environment. This group is stabilized by charge−charge interactions with the side chains of Glu127 and Asp184, and by the proximity of Asn171(O_{δ}) and Glu170(O_{CO}). The presence of a positive charge at this location is important for binding, as evidenced by the decreased affinity of inhibitors related to H8 where the spacing between the sulfonamide and ammonium groups is progressively increased from two to five carbons (*16*). The spatial congruence of balanol, H-series inhibitors, and Mg_2ATP at the level of the adenine-binding pocket was noted previously (*24*, *30*, *38*).

In the present study, we use a theoretical model to establish a link between three-dimensional crystal structures of cAPK: ligand complexes and the thermodynamics of ligand binding, the former topic being more thoroughly discussed in an accompanying report (*24*). We calculate the differential binding affinities of three classes of ligands (Table 1) toward the C subunit of cAPK, using previously determined structures (*24*, *30*, *33*). Binding affinities are obtained from a thermodynamic cycle based on continuum electrostatics and a surface-area-dependent nonpolar term. The usefulness of such implicit-solvent models as a tool for the theoretical study of biomolecular systems has been shown by many groups (*39*−*45*). Applications include the calculation of hydration or transfer free energies (*46*−*48*), the estimation of protein−ligand binding free energies (*49*−*51*), the calculation of acid−base properties of macromolecules (*52*, *53*), and the study of solvent effects on conformation (*54*−*58*).

[2] The hydrogen bonds reported in ref *24* are inferred from atomic distances and angles measured in the crystal structure. In the present calculations, hydrogens are placed explicitly and the complex is energy minimized (see Computational Procedures), resulting in slight conformational changes. The hydrogen bonds observed in the energy-minimized structure are identical to those described in ref *24* with a single exception: the 6″-hydroxyl group of balanol forms an intramolecular hydrogen bond with the oxygen of the ketone linkage in the benzophenone moiety.

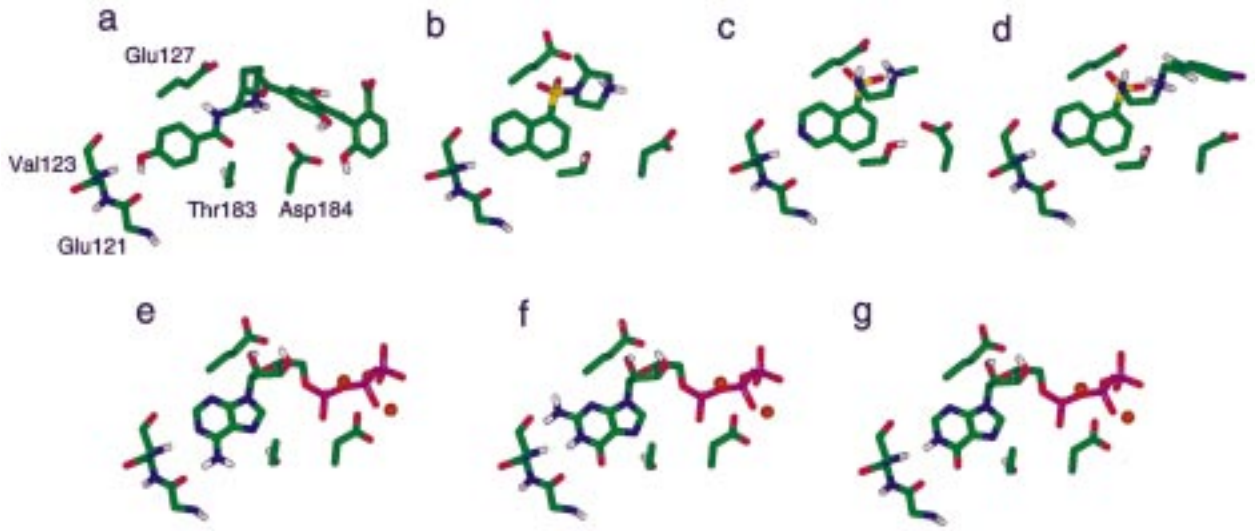

FIGURE 2: Energy-minimized structures (active sites) of the binary complexes between the C subunit and the ligands considered in this study. Residues forming hydrogen bonds to the nucleotide base or the inhibitor group mimicking it are displayed, as well as Glu127 and Asp184, which stabilize a positive magnesium or ammonium group. Residues involved in polar interactions with other parts of the ligand are not displayed; (a) balanol; (b) H7; (c) H8; (d) H89; (e) Mg_2ATP; (f) Mg_2GTP; (g) Mg_2ITP.

Table 1: Experimental and Calculated Binding Free Energies of cAPK Ligands[a]

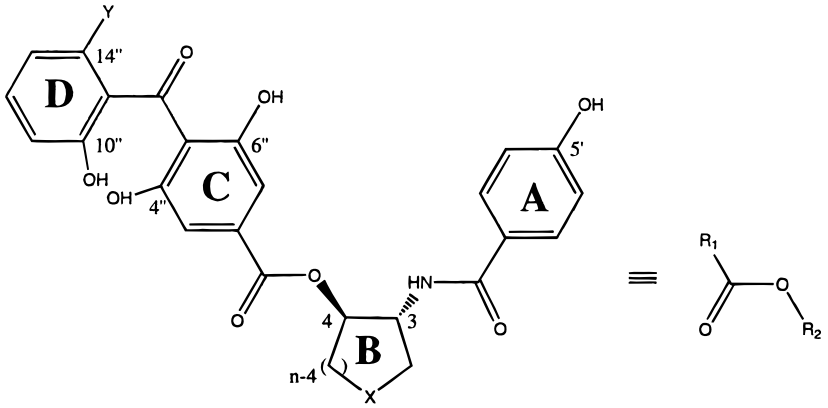

	compd	*n*	*X*	*Y*	*Q*	K_i	ΔG_{exp}	ΔG_{calc}	ΔG_{np}	ΔG_{el}
1	(−)-balanol	7	NH_2^+	COO^-	+1/−1	0.05/0.0047[b]	−10.0/−11.4	−25.9	−27.4	1.5
2	R_1-COOMe fragment			COO^-	−1	>1[c]	>−8.2	−15.0	−17.5	2.5
3	R_2-OH fragment	7	NH_2^+	H	+1	>1[c]	>−8.2	−17.0	−15.5	−1.5
4	ether analog	7	O	COO^-	−1	0.45[d]	−8.7	−22.0	−27.5	5.4
5	sulfide analog	7	S	COO^-	−1	7.5[d]	−7.0	−21.6	−27.6	6.0
6	sulfone analog	7	SO_2	COO^-	−1	38[d]	−6.1	−21.5	−27.9	6.4
7	carbocyclic analog	7	CH_2	COO^-	−1	1.4[d]	−8.0	−22.0	−27.6	5.7
8	10″-deoxybalanol	7	NH_2^+	COO^-	+1/−1	0.0039[c]	−11.5	−26.1	−27.2	1.1
9	5′-deoxybalanol	7	NH_2^+	COO^-	+1/−1	0.0035[c]	−11.6	−25.8	−26.9	1.1
10	4″,6″-dideoxybalanol	7	NH_2^+	COO^-	+1/−1	0.0034[c]	−11.6	−25.7	−27.1	1.4
11	piperidine analog	6	NH_2^+	COO^-	+1/−1	0.35[d]	−8.9	−26.0	−26.6	0.6
12	pyrrolidine analog	5	NH_2^+	COO^-	+1/−1	0.07[d]	−9.8	−26.1	−26.1	0.1
13	cyclopentane analog	5	CH_2	COO^-	−1	0.03[d]	−10.3	−20.9	−26.6	5.7
14	H7 inhibitor				+1	3.0[e]	−7.6	−18.9	−16.7	−2.2
15	H8 inhibitor				+1	1.2[e]	−8.1	−19.9	−15.3	−4.6
16	H89 inhibitor				+1	0.048[e]	−10.0	−22.3	−21.8	−0.5
17	Mg_2ATP				+4/−4	10[f]	−6.9	−21.6	−22.9	1.3
18	Mg_2GTP				+4/−4	3700[f]	−3.3	−17.6	−23.4	5.8
19	Mg_2ITP				+4/−4	14 200[f]	−2.5	−18.7	−22.7	4.0

[a] *n*, number of atoms in ring B; *Q*, total charge of the ligand, +1/−1 and +4/−4 indicate zwitterions with the corresponding charge separation; K_i: inhibition (or dissociation) constant in micromolarity; ΔG_{exp}, experimental binding free energy in kilocalories per mole, calculated from K_i at 300 K; ΔG_{calc}, ΔG_{np} and ΔG_{el}, calculated binding free energy, and the nonpolar and electrostatic contributions to this number. [b] Data from ref *13* (first number, ref *12* reports a nearly equivalent value of 0.04 μM) or from ref *14* (second number). [c] Data from ref *14*. [d] Data from ref *13*. [e] Data from ref *16*. [f] Data from ref *20*.

These methods are very attractive because they give a quite accurate description of solvent effects at a reasonable computational cost (*59*). They also avoid the sampling problems often associated with explicit-solvent methods.

Similar continuum calculations were already performed on the C subunit of cAPK to study the thermodynamics of the open/closed conformational transition and the influence of ATP and PKI(5−24) binding on this equilibrium (*60*), to study the electrostatic interactions involved in the recognition of the arginine-rich consensus sequence in peptide substrates (*61*, *62*), and to identify the complementary surface patches on the catalytic and regulatory subunits (*63*). As shown below, the implicit solvent model used in the present study reproduces most of the experimental binding free energy trends, and provides insight into factors determining the affinity and specificity of ligand binding to cAPK.

COMPUTATIONAL PROCEDURES

The present calculations of binding affinities rely on the assumption that the statistical ensemble of conformations and charge states accessible to a solvated solute may be represented by a single predominant conformation and charge state. The free energy of the solute−solvent system is then partitioned into an electrostatic and a nonpolar contribution

$$G = G_{el} + G_{np}$$

We define the reference state of the system ($G = 0$) as the state where all the solute atomic partial charges are set to zero and the solvent is a liquid alkane. The electrostatic term, G_{el}, is the sum of the work required to assemble the solute charges in a homogeneous medium of permittivity ϵ_i (Coulomb contribution, G_{Cb}), plus the work required to change the external permittivity from ϵ_i to ϵ_w (reaction-field contribution, G_{RF}), where ϵ_i and ϵ_w are the solute (internal) and solvent (water) dielectric permittivities, respectively. The Coulomb contribution, G_{Cb}, is calculated as

$$G_{Cb} = \frac{1}{4\pi\epsilon_o\epsilon_i}\frac{1}{2}\sum_{i,j\neq i}\frac{q_i q_j}{r_{ij}} \qquad (2)$$

The reaction-field contribution, G_{RF}, is obtained numerically from a finite-difference solution to the electrostatic potential defined by the Poisson equation, and a Green's function correction (*45*). The nonpolar contribution, G_{np}, is the work required to transfer the uncharged solute from the alkane solvent into water. It is assumed to be proportional to the area of the solute−solvent boundary through an empirical coefficient γ (effective microscopic interfacial tension). This term should encompass the "hydrophobic" effect as well as van der Waals (dispersion) interactions. In practice, γ is calibrated to reproduce experimental transfer free energies of alkane molecules (assumed uncharged) from the liquid alkane phase into water (*46*). The binding free energy of a protein:ligand complex in aqueous solution is calculated from the thermodynamic cycle represented in Figure 3 (*40*, *49*, *64*). The apoprotein and the ligand are first discharged in water (step 1) and transferred into an alkane solvent (step 2). The two molecules are associated in their reference states (step 3). Finally, the uncharged binary complex is transferred into water (step 4) and charged (step 5). If the free-energy change for the association of apolar (alkane-like) molecules in an alkane phase, ΔG_{alk}, is assumed to be zero, we have

$$\Delta G_{calc} = \Delta G_{el} + \Delta G_{np} = \Delta G_{Cb} + \Delta G_{RF} + \Delta G_{np}$$

where ΔG_x stands for $G_x^{bin} - G_x^{apo} - G_x^{lig}$, apo, lig, and bin denoting the apoprotein, the free ligand, and the binary complex, respectively.

The ligands considered in this study are listed in Table 1. All calculations are based on a single energy-minimized conformation of the binary complex, assumed predominant in all thermodynamic states. For the different ligands, these conformations were modeled using the 1BX6 (*24*) (balanol and derivatives), 1YDR (*30*) (H7), 1YDS (*30*) (H8), 1YDT (*30*) (H89), and 1ATP (*27*) (ATP analogues) structures as deposited in the Brookhaven protein data bank. PKI(5−24) (the I chain in the PDB files), and crystallographic water molecules were deleted wherever present. All residues were protonated according to the ionization state of the isolated amino acid at pH 7. The terminal carboxylate group was considered ionized but the amino group of the first protein residue visible in the crystallographic structure was kept neutral, since it is not the N-terminus of the protein. The phosphorylated residues P-Thr197 and P-Ser338 were modeled as singly protonated. The positions of the hydrogen atoms on the neutral histidine residues and on the phosphate groups were determined by visual inspection of the environment of the residues in the different structures. The 14″-group (benzoic acid: $pK_a \approx 4.2$) and the cyclic secondary amine ($pK_a \approx 11$) of balanol derivatives, as well as the secondary amine [$pK_a = 8.9$ in H8 (*16*)] of H-series inhibitors were considered ionized. For Mg_2ATP and analogues, the magnesium ions were treated as an integral part of the ligand. The commercial version of the united-atom CHARMm22 force field (*65*) was used for all calculations. Missing ligand parameters were derived by analogy with existing fragments in the force-field library. Partial atomic charges for the isoquinoline and hypoxanthine fragments[3] were calculated from an ab initio HF/6-31G** geometry optimization using Gaussian94 (*66*) and a CHELPG (*67*) electrostatic potential fit with dipole moment constraint on the optimized structure. The sulfonamide or ribose moieties were replaced by a hydrogen atom for these calculations. Charges obtained for the apolar hydrogens, and for the N9 hydrogen of hypoxanthine, were summed into those of the atom bearing the hydrogen. The charges obtained by this procedure were scaled by a factor 0.8 to improve the compatibility with other CHARMm parameters (*68*). To check the validity of this procedure, two tests were performed. First, the calculations for the C:H89 and the C:ITP complexes were repeated with unscaled charges, and the results found to change by only 0.2 and 0.3 kcal/mol, respectively. Second, charges were generated for adenine and guanine using the same procedure and compared to the CHARMm charges. The charges deviated on average by 0.10*e* and 0.05*e*, respectively, with a few deviations above 0.1*e* and none above 0.2*e*.

For each ligand considered, initial coordinates were generated for the binary C:ligand complexes using available crystallographic coordinates. Coordinates for the polar hydrogens were generated using the CHARMm HBUILD (*69*) module, and refined by energy minimization, keeping

[3] The charges (*e*) used for isoquinoline are −0.18 (C_5), 0.08 (C_6), −0.01 (C_7), −0.02 (C_8), −0.13 (C_9), 0.42 (C_{10}), −0.32 (C_{11}), 0.37 (C_{12}), −0.52 (N_{13}), and 0.31 (C_{14}). The charges used for hypoxanthine are −0.647 (N_1), 0.333 (H_1), 0.522 (C_2), −0.603 (N_3), 0.528 (C_4), −0.052 (C_5), 0.662 (C_6), −0.490 (O_6), −0.446 (N_7), 0.362 (C_8), and −0.214 (N_9).

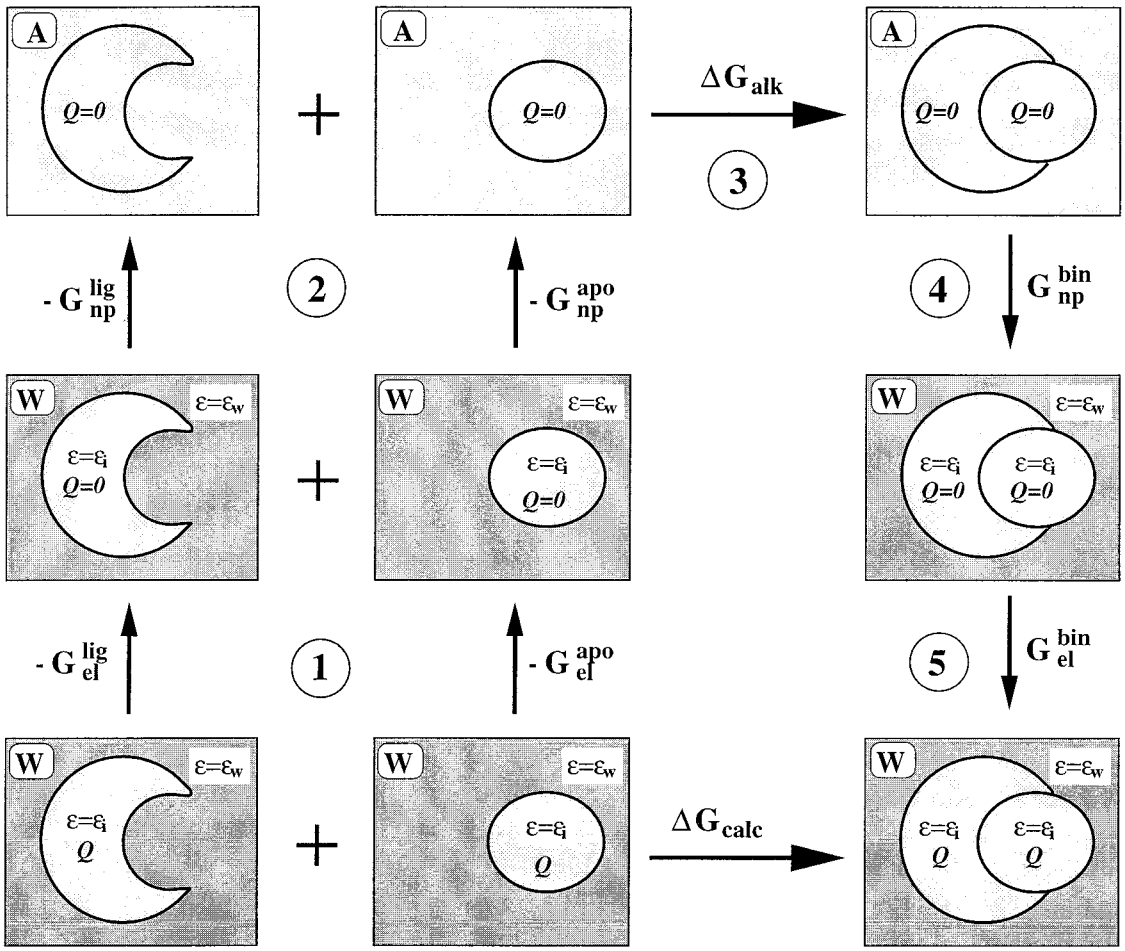

FIGURE 3: Thermodynamic cycle used for calculating the binding free energy. For each diagram, the inset at the upper left represents the nature of the solvent (A = alkane, W = water), Q denotes collectively the charges of the solute atoms ($Q = 0$ indicates that the solute atomic partial charges are set to zero), and ϵ is the relative dielectric permittivity of the medium. Starting from the bottom left, the apoprotein and the ligand are discharged in water (step 1, $\Delta G = -G_{el}^{apo} - G_{el}^{lig}$), transferred into a liquid alkane (step 2, $\Delta G = -G_{np}^{apo} - G_{np}^{lig}$), and associated (step 3, $\Delta G_{alk} = 0$). The uncharged binary complex is then transferred into water (step 4, $\Delta G = G_{bin}^{np}$), and charged (step 5, $\Delta G = G_{bin}^{el}$). Here, apo, lig, and bin denote the apoprotein, the free ligand, and the binary complex, respectively.

all non-hydrogen atoms fixed. A short (100 steps conjugate gradient) energy minimization of the complex was then performed, followed by extensive optimization of the ligand with fixed protein atoms, in both cases using a distance-dependent dielectric constant $\epsilon = 5r$. Finally, the complex was rotated to be inscribed optimally in a cubic box, and the free energies of the complex, the apoprotein and the ligand were calculated with the UHBD program (*45*, *70*, *71*), using a 240 × 240 × 240 points grid with 0.3 Å spacing, a molecular surface defined by rolling a probe of 1.4 Å radius on the molecule (*72*), together with $\epsilon_i = 2$ (liquid alkane), $\epsilon_w = 78$ (water) and $\gamma = 0.025$ kcal/(mol Å^2) (*42*, *46*). The choice of the grid parameters left a void of at least 5 Å on all sides of the complex, and has led to well converged results for the hydration free energies in this particular system (*60*).

RESULTS

Contributions to the Binding Free Energy. Table 1 lists experimental and calculated binding free energies for the C:ligand complexes together with the nonpolar (ΔG_{np}) and electrostatic (ΔG_{el}) contributions to the calculated numbers. Uncertainities in the experimental values, which are gathered from five different sources and may correspond to somewhat different assays, should not be overlooked. For example, the value of ΔG_{exp} reported for balanol varies by 1.4 kcal/mol depending on the source (*12*−*14*). We note in particular the following causes of uncertainities: (i) it is not always clear whether the reported K_is describe the affinity of the ligand for the C-subunit or for a C:peptide complex, since kinetic assays involve the presence of a peptide substrate (*16*); (ii) the presence of ATP and magnesium during the assay may induce a dependence on the Mg^{2+} concentration (*19*); (iii) some of the assays are performed using enantiomerically pure ligands, whereas others involve racemic mixtures.

Both experimental and theoretical values relative to those for balanol ($\Delta\Delta G$) are displayed in Figure 4. Our calculations reproduce the experimental range of binding free energies ($\Delta\Delta G_{calc}$ versus $\Delta\Delta G_{exp}$). The range of $\Delta\Delta G_{calc}$ (−0.4 to +10.9 kcal/mol) may appear wide from a practical point of view, yet this range is actually very narrow considering the magnitudes of the individual contributions to this number. The contributions G_{Cb}, G_{RF}, and G_{np} to the solvation free energy of the apoprotein or the binary complexes are on the order of -7×10^3, -3×10^3 and 4×10^2 kcal/mol, respectively. These numbers cancel to a large extent around the thermodynamic cycle (Figure 3), and ΔG_{Cb}, ΔG_{RF}, and ΔG_{np} are in narrower ranges (−28.0 to −198.7, +30.5 to

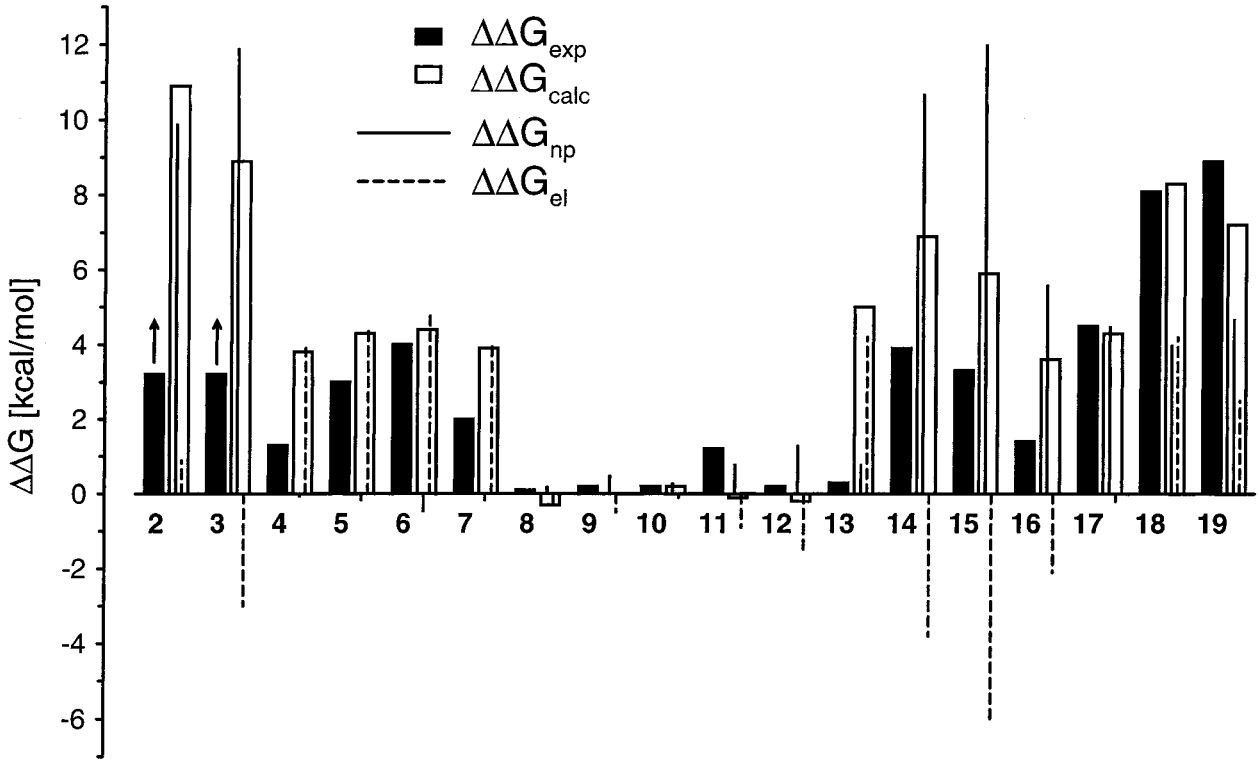

FIGURE 4: Experimental and calculated binding free energies relative to balanol; $\Delta\Delta G_{exp}$: experimental difference $\Delta G_{exp}(\mathbf{X}) - \Delta G_{exp}(\mathbf{1})$, where $\Delta G_{exp}(\mathbf{X})$ is the experimental binding free energy for a given ligand **X** (**X** = **2**−**19**, see Table 1) and $\Delta G_{exp}(\mathbf{1})$ is the experimental binding free energy for **1** reported by the same authors (or in ref *14* if not available). $\Delta\Delta G_{calc}$: calculated value $\Delta G_{calc}(\mathbf{X}) - \Delta G_{calc}(\mathbf{1})$; $\Delta\Delta G_{np}$ and $\Delta\Delta G_{el}$ are the nonpolar and electrostatic contributions to $\Delta\Delta G_{calc}$, i.e., $\Delta\Delta G_{calc} = \Delta\Delta G_{np} + \Delta\Delta G_{el}$; arrows indicate that the experimental value is a lower bound.

+200.0, and −27.9 to −15.3 kcal/mol, respectively). A second large cancellation occurs when ΔG_{Cb} and ΔG_{RF} are combined into ΔG_{el}, which varies in the range −2.2 to +6.4 kcal/mol. Thus, the observed variations in $\Delta\Delta G_{calc}$ arise from the cancellation of contributions which are 10^3−10^4 times larger. Consequently, the uncertainity in $\Delta\Delta G_{calc}$ is likely to increase rapidly with the level of structural differences between a given inhibitor and balanol.

The calculated binding free energies are more favorable by about 15 kcal/mol than the experimental ones (Table 1), primarily due to the loss of translational and rotational entropy associated with the binding process not being accounted for in the model (*73*). The corresponding unfavorable contributions have been estimated to 7−15 kcal/mol for the binding of small ligands to proteins and 0.5−1 kcal/mol per frozen (protein or ligand) internal rotation (*74*−*78*). The possible release or freezing of tightly bound solvent molecules may also lead to an entropic contribution (*44*, *73*). Ligand binding may also induce some strain (ligand compression) which would appear as an unfavorable contribution in the van der Waals and covalent force-field energy terms. Since these are not included in the present calculations, this strain contribution does not appear in ΔG_{calc}. Finally, the C subunit may assume open, intermediate, and closed conformations (*24*, *25*, *28*, *29*, *35*, *36*). If ligand binding induces a conformational transition (induced fit), the corresponding free-energy contribution will not be accounted for in ΔG_{calc}. This contribution may be small (*79*), but its exact magnitude is currently unknown. We assume here that these neglected contributions are of similar magnitudes for all C:ligand complexes and may be of the order of 15 kcal/mol. The general picture emerging from the results presented in Table 1 is that binding is driven by nonpolar interactions,[4] partly opposed by the neglected (mostly entropic) contributions, whereas electrostatic interactions play a minor role in determining the overall binding affinity. However, since ΔG_{np} is weakly selective between inhibitors of a similar size, ΔG_{el} plays an important role in determining the binding specificity. These key principles, which are consistent with the conclusions of previous studies (*42*, *43*), are illustrated below by reference to specific examples of C:ligand complexes.

Balanol Derivatives. In agreement with experimental results, the benzophenone (**2**) and the hexahydroazepine (**3**) fragments derived from balanol are calculated to bind very poorly to the C subunit compared to balanol. This is due to a less favorable nonpolar term, which is a consequence of the smaller size of these inhibitors. Note, however, that the $\Delta\Delta G_{calc}$ values are probably upper bounds to the experimental values since the entropic cost is likely to be lower for the binding of a smaller inhibitor with a reduced number of free internal rotations. The $\Delta\Delta G_{calc}$ values for compounds in which the ammonium group of ring B in balanol (**1**) is replaced by a neutral ether (**4**), sulfide (**5**), sulfone (**6**), or methylene (**7**) group are somewhat higher than experimentally determined values, but the correct ranking in the series **1**, **4**−**7** is reproduced. The decreased affinity of compounds **4**−**7** arises from less favorable electrostatics and can be traced to the loss of charge−charge interaction between the

[4] The present model does not distinguish between hydrophobic and van der Waals contributions to the nonpolar term. The hydrophobic contribution is likely to be dominant, since van der Waals interactions exist both in the bound state (within the complex) and unbound state (with water), leading to partial cancellation (*43*).

ammonium group and the carboxylates of Glu127 and Asp184. It has been suggested that the observed trends may arise from changes in the conformation of the relatively flexible seven-membered ring B (*13*). In our simple modeling of analogues **4**−**7**, no significant conformational changes with respect to **1** were observed in the bound ligand after minimization. Thus, although the present calculations cannot rule out a role of conformational effects, the trends observed experimentally can be rationalized on the basis of purely electrostatic effects.

The deoxy compounds **8**−**10** have similar affinities toward the C subunit compared to balanol, which is in agreement with the experimental results. This may appear surprising, since all hydroxyl groups of balanol with the exception[2] of the 6″-hydroxyl are involved in hydrogen bonds with the protein. In particular, all structures solved to date of cAPK complexes involving inhibitors competing with ATP contain at least one hydrogen bond between the ligand and backbone amides in the linker region (*24*, *25*, *30*−*32*, *38*). The 5′-hydroxyl of balanol might, therefore, seem essential for high-affinity binding. To understand why this is not the case, one may define contributions of individual groups to the binding free energy of balanol in terms of interaction ($\Delta\Delta G_{inter}$) and desolvation ($\Delta\Delta G_{desolv}$) components.[5] For the 5′-, 10″-, 4″- and 6″-hydroxyl groups, we calculate $\Delta\Delta G_{inter}$ to be −3.5, −1.0, −1.1, and 0.4 kcal/mol, respectively. Thus, hydrogen-bonding hydroxyl groups (all except the 6″-hydroxyl) indeed promote complex formation by their favorable interaction with the protein. However, this favorable contribution is canceled by the desolvation penalty $\Delta\Delta G_{desolv}$ (3.5, 1.3, 0.9, and 0.0 kcal/mol, respectively) associated with the removal of the interacting partners from water. These examples illustrate that formation of hydrogen bonds in these complexes represents a negligible contribution to the binding affinity, because it is accompanied by the desolvation of the two hydrogen-bonding groups (*42*, *43*). However, it is unfavorable to desolvate polar groups without forming a hydrogen bond in the complex. Consequently, the disposition of hydrogen-bonding groups in the protein active site and in the ligand is crucial for the binding specificity of a ligand toward different proteins or of a protein toward different ligands.

Compounds **11** and **12**, in which the number of atoms in ring B is changed from seven (**1**) to six (**11**) or to five (**12**), pose a more difficult conformational problem. $\Delta\Delta G_{el}$ may be sensitive to the choice of a specific ring conformation. Among a number of possible conformations, we report the results for those with the lowest internal (covalent) energy after minimization. Variations in strain and entropic contributions with the ring size are also likely to be significant. Consequently, the uncertainity in $\Delta\Delta G_{calc}$ for these compounds may be quite large. Nevertheless, the calculated values agree reasonably well with experimental values. The experimentally determined binding free energy of the cyclopentane analogue **13** is slightly more negative than that of balanol. In contrast, the calculated value for **13** is less negative by 5 kcal/mol, due to a large, positive $\Delta\Delta G_{el}$. This result is, however, consistent with that obtained for compound **7** (same $\Delta\Delta G_{el}$, $\Delta\Delta G_{np}$ lower by 1 kcal/mol), and it is puzzling that $\Delta\Delta G_{calc}$ is essentially correct for **7** but incorrect for **13**. This points toward effects not accounted for in the present model, such as significant conformational differences between **7** and **13** in the binary complex or in the unbound ligand, or different interactions with specific water molecules.

H-Series Inhibitors. The $\Delta\Delta G_{calc}$ values for the H-series inhibitors (**14**−**16**) are 2−3 kcal/mol higher than their experimental counterparts. Although these inhibitors differ more significantly from balanol in their structures than the balanol derivatives considered above (in particular in the number of free internal rotations), the trends among H7, H8, and H89 are reproduced correctly. The calculated differences in binding affinities between H7 and H89 (3.3 kcal/mol) and between H8 and H89 (2.3 kcal/mol) are close to the experimentally determined differences of 2.4 and 1.9 kcal/mol, respectively. While $\Delta\Delta G_{np}$ is generally small for the balanol derivatives, it is positive and large for the H-series inhibitors, because they occupy a smaller portion of the enzyme active site. On the other hand, unlike all balanol derivatives except **3**, H-series inhibitors display a favorable electrostatic contribution to binding, which may seem surprising since these compounds form fewer polar contacts with the protein in the complex (*30*, *38*). The reason is that, although the electrostatic contribution to interaction[5] is 44−51 kcal/mol less favorable for H-series inhibitors than for balanol, the desolvation penalty is less unfavorable by 50−53 kcal/mol. Thus, H-series inhibitors occupy the active-site cavity only partially and form few hydrogen bonds with the enzyme, but these inhibitors still bind with high affinity because their less polar character makes their desolvation easier. This observation suggests that a tighter binding inhibitor might be constructed by replacing the *p*-hydroxybenzamide ring of balanol (ring A) by the isoquinolinesulfonamide group of the H-series inhibitors, i.e., connecting by a bond the C3 carbon of balanol (Figure 1a) to the sulfonamide nitrogen of H7 (Figure 1b). This hybrid inhibitor could be modeled in a reasonable covalent geometry using the C:balanol (*24*) and C:PKI(5−24):H7 (*30*) crystal structures. The calculated binding free energy for this inhibitor relative to balanol is $\Delta\Delta G_{calc} = -1.8$ kcal/mol, which would make of this compound the most potent cAPK inhibitor known to date. This suggestion awaits experimental confirmation.

ATP Analogues. The values of $\Delta\Delta G_{calc}$ for Mg_2ATP analogues (**17**−**19**) agree well with experimental numbers, except for an inversion between Mg_2GTP and Mg_2ITP. For these three compounds, $\Delta\Delta G_{np}$ is positive and of similar magnitude. Despite the larger number of polar contacts with the protein for Mg_2ATP analogues than for balanol, ΔG_{el} is either close to zero (Mg_2ATP) or unfavorable (Mg_2GTP, Mg_2ITP). The electrostatic contribution to interaction[5] is much more favorable for Mg_2ATP than for balanol (by 581 kcal/mol), but the desolvation contribution completely cancels out this effect. Thus, Mg_2ATP binds with lower affinity compared to balanol, essentially because it occupies a smaller portion of the active-site cavity. The experimental selectivity between Mg_2ATP, Mg_2GTP and Mg_2ITP can be rationalized structurally, see Figure 2, panels e−g. Adenine

[5] The definitions are $\Delta\Delta G_{inter} = [G^{bin}(\mathbf{1}) - G^{apo}(\mathbf{1})] - [G^{bin}(\boldsymbol{X}) - G^{apo}(\boldsymbol{X})]$ and $\Delta\Delta G_{desolv} = -[G^{lig}(\mathbf{1}) - G^{lig}(\mathbf{X})]$, where **X** is the ligand of interest, apo denotes the apoprotein, bin the binary complex, and lig the free ligand. Thus, $\Delta\Delta G_{calc} = \Delta\Delta G_{inter} + \Delta\Delta G_{desolv}$. For compounds **8**−**10**, both interaction and desolvation components are almost exclusively electrostatic in nature.

forms two hydrogen bonds to backbone amides in the linker region [N6 to Gly121 (O_{CO}) and Val123(H_{NH}) to N1]. In the case of Mg_2ITP, the N6 nitrogen of Mg_2ATP is replaced by an oxygen and the N1 nitrogen now bears a hydrogen. The polarity inversion of these two groups strongly destabilizes the complex. For Mg_2GTP, the additional amino group at position 2 may form a hydrogen bond to Val123(O_{CO}). In the calculations, unlike in the experimental result, this interaction does not compensate for the desolvation penalty associated with the removal of this additional amino group from water.

DISCUSSION

The implicit-solvent model used in the present study reproduces most of the trends in binding free energy observed experimentally. The following general observations can be made with respect to the binding of the three classes of cAPK ligands considered. (i) Binding is driven by nonpolar (hydrophobic and van der Waals[4]) interactions, and binding affinity correlates primarily with the degree to which the ligand fills the active-site cavity (shape complementarity). (ii) For inhibitors of similar sizes, electrostatic interactions are significant determinants of the binding specificity, as is apparent from the series of balanol derivatives **1**, **4**−**7**, and the series of nucleotides **17**−**19**. (iii) The calculated binding affinities are sensitive to the overall charge or charge distribution of the ligand. Due to electrostatic screening by the solvent, this dependence is, however, by 1−2 orders of magnitude smaller than the vacuum (Coulomb) contribution. We observe a systematic dependence of the (solvent-screened) electrostatic contribution on the overall charge of the ligand. Positively charged ligands (**3** and **14**−**16**) have a negative ΔG_{el}, whereas negatively charged ligands (**2**, **4**−**7**, and **13**) have a positive and large ΔG_{el} (about 6 kcal/mol). Zwitterionic inhibitors (**1**, **8**−**12**, and **17**−**19**) share a positive ΔG_{el} of smaller magnitude. The presence of a positive charge in balanol and in the H-series inhibitors is thus important for tight binding. (iv) Besides this dependence on the overall charge of the ligand, the electrostatic contribution does not correlate with the number of hydrogen bonds formed in a particular complex, because the desolvation cost associated with the removal of hydrogen-bonding groups from water balances the free energy gained by the formation of hydrogen bonds in the complex. On the other hand, hydrogen-bonding groups that must be desolvated but cannot form hydrogen bonds in the complex contribute unfavorably to the binding free energy, as illustrated by Mg_2ITP and Mg_2GTP; (v) The electrostatic contribution favors the binding of compounds that are poorly solvated but can make specific hydrogen bonds in the complex, as is the case for the isoquinoline ring of the H-series inhibitors.

According to these five criteria, balanol is the best nonpolar binder. Although H-series inhibitors are poorer nonpolar binders, they still exhibit overall tight binding due to the smaller desolvation penalties for these compounds. Mg_2ATP binds with an electrostatic contribution similar to that of balanol, but Mg_2ATP is a poorer nonpolar binder, with, therefore, a lower overall affinity for the free C subunit. Finally, our calculations suggest that a hybrid compound constructed by replacing the ring A of balanol by the isoquinolinesulfonamide group of H-series inhibitors may be a more potent cAPK inhibitor than any of those known to date.

The present study demonstrates that it is possible, using theoretical tools, to calculate the relative affinities of a broad spectrum of ligands toward the C subunit of cAPK with a reasonable accuracy. Although absolute binding free energies cannot be obtained, the method is able to reproduce many of the qualitative trends observed experimentally. Rather than to replace an experimental measurement, the specific power of these calculations is to provide a qualitative understanding of the driving forces responsible for the binding of specific inhibitors. Reaching such an understanding is an important first step toward the rational design of potent and specific kinase inhibitors.

ACKNOWLEDGMENT

We thank T. C. Diller and A. H. Elcock for helpful discussions and their critical reading of the manuscript.

REFERENCES

1. Taylor, S. S., Buechler, R. A., and Yonemoto, W. (1990) *Annu. Rev. Biochem. 59*, 971.
2. Hanks, S. K., Quinn, A. M., and Hunter, T. (1988) *Science 241*, 42.
3. Hanks, S. K., and Hunter, T. (1995) *FASEB J. 9*, 576.
4. Walsh, D. A., Perkins, J. P., and Krebs, E. G. (1968) *J. Biol. Chem. 243*, 3763.
5. Montminy, M. R., Gonzalez, G. A., and Yamamoto, K. K. (1990) *Trends Neurosci. 13*, 184.
6. Frank, D. A., and Greenberg, M. E. (1994) *Cell 79*, 5.
7. Kato, J.-Y., Matsuoka, M., Polyak, K., Massague, J., and Sherr, C. J. (1994) *Cell 79*, 487.
8. Grieco, D., Procellimi, A., Avvedimento, E. V., and Gottesman, M. E. (1996) *Science 271*, 1718.
9. Pepinsky, R. B., and Sinclair, L. K. (1986) *Nature 321*, 81.
10. Tritton, T. R., and Hickman, J. A. (1990) *Cancer Cells 2*, 95.
11. Ishii, H., Jirousek, M. R., Koya, D., Takagi, C., Xia, P., Clermont, A., Bursell, S.-E., Kern, T. S., Ballas, L. M., Heath, W. F., Stramm, L. E., Feener, E. P., and King, G. L. (1996) *Science 272*, 728.
12. Defauw, J. M., Murphy, M. M., Jagdmann, G. E., Jr., Hu, H., Lampe, J. W., Hollinshead, S. P., Mitchell, T. J., Crane, H. M., Heerding, J. M., Mendoza, J. S., Davis, J. E., Darges, J. W., Hubbard, F. R., and Hall, S. E. (1996) *J. Med. Chem. 39*, 5215.
13. Lai, Y.-S., Mendoza, J. S., Jagdmann, G. E., Jr., Menaldino, D. S., Biggers, C. K., Heerding, J. M., Wilson, J. W., Hall, S. E., Jiang, J. B., Janzen, W. P., and Ballas, L. M. (1997) *J. Med. Chem. 40*, 226.
14. Koide, K., Bunnage, M. E., Paloma, L. G., Kanter, J. R., Taylor, S. S., Brunton, L. L., and Nicolaou, K. C. (1995) *Chem. Biol. 2*, 601.
15. Setyawan, J., Koide, K., Diller, T. C., Taylor, S. S., Nicolaou, K. C., and Brunton, L. (Manuscript in preparation).
16. Hidaka, H., Inagaki, M., Kawamoto, S., and Sasaki, Y. (1984) *Biochemistry 23*, 5036.
17. Chijiwa, T., Mishima, A., Hagiwara, M., Sano, M., Hayashi, K., Inoue, T., Naito, K., Toshioka, T., and Hidaka, H. (1990) *J. Biol. Chem. 265*, 5267.
18. Lew, J., Coruh, N., Tsingely, I., Garrod, S., and Taylor, S. S. (1997) *J. Biol. Chem. 272*, 1507.
19. Cook, P. F., Neville Jr., M. E., Vrana, K. E., Hartl, F. T., and Roskoski, R., Jr. (1982) *Biochemistry 21*, 5794.
20. Bhatnagar, D., Roskoski, R., Jr., Rosendahl, M. S., and Leonard, N. J. (1983) *Biochemistry 22*, 6310.
21. Cheng, H.-C., van Patten, S. M., Smith, A. J., and Walsh, D. A. (1985) *Biochem. J. 231*, 655.
22. Whitehouse, S., and Walsh, D. A. (1983) *J. Biol. Chem. 258*, 3682.

23. Herberg, F. W., and Taylor, S. S. (1993) *Biochemistry 32*, 14015.
24. Narayana, N., Diller, T. C., Koide, K., Nicolaou, K. C., Brunton, L. L., Xuong, N.-H., Ten Eyck, L. F., and Taylor, S. S. (1999) *Biochemistry 38*, 2367−2376.
25. Narayana, N., Cox, S., Xuong, N.-H., Ten Eyck, L. F., and Taylor, S. S. (1997) *Structure 5*, 921.
26. Knighton, D. R., Zheng, J., Ten Eyck, L. F., Ashford, V. A., Xuong, N.-H., Taylor, S. S., and Sowadski, J. M. (1991) *Science 253*, 407.
27. Zheng, J., Knighton, D. R., Ten Eyck, L. F., Karlsson, R., Xuong, N.-H., Taylor, S. S., and Sowadski, J. M. (1993) *Biochemistry 32*, 2154.
28. Karlsson, R., Zheng, J., Xuong, N.-H., Taylor, S. S., and Sowadski, J. M. (1993) *Acta Crystallogr., Sect. D 49*, 381.
29. Zheng, J., Knighton, D. R., Xuong, N.-H., Taylor, S. S., Sowadski, J. M., and Ten Eyck, L. F. (1993) *Protein Sci. 2*, 1559.
30. Engh, R. A., Girod, A., Kinzel, V., Huber, R., and Bossemeyer, D. (1996) *J. Biol. Chem. 271*, 26157.
31. Bossemeyer, D., Engh, R. A., Kinzel, V., Ponstingl, H., and Huber, R. (1993) *EMBO J. 12*, 849.
32. Prade, L., Engh, R. A., Girod, A., Kinzel, V., Huber, R., and Bossemeyer, D. (1997) *Structure 5*, 1627.
33. Zheng, J., Trafny, E. A., Knighton, D. R., Xuong, N.-H., Taylor, S. S., Ten Eyck, L. F., and Sowadski, J. M. (1993) *Acta Crystallogr., Sect. D 49*, 362.
34. Knighton, D. R., Xuong, N.-H., Taylor, S. S., and Sowadski, J. M. (1991) *J. Mol. Biol. 220*, 217.
35. Knighton, D. R., Bell, S. M., Zheng, J., Ten Eyck, L. F., Xuong, N.-H., Taylor, S. S., and Sowadski, J. M. (1993) *Acta Crystallogr., Sect. D 49*, 357.
36. Karlsson, R., Madhusudan, Taylor, S. S., and Sowadski, J. M. (1994) *Acta Crystallogr., Sect. D 50*, 657.
37. Hemmer, W., McGlone, M., Tsingely, I., and Taylor, S. S. (1997) *J. Biol. Chem. 272*, 16946.
38. Taylor, S. S., and Radzio-Andzelm, E. (1997) *Curr. Opin. Chem. Biol. 1*, 219.
39. Warwicker, J., and Watson, H. C. (1982) *J. Mol. Biol. 157*, 671.
40. Gilson, M. K., and Honig, B. (1988) *Proteins: Struct., Funct., Genet. 4*, 7.
41. Zacharias, M., Luty, B. A., Davis, M. E., and McCammon, J. A. (1994) *J. Mol. Biol. 238*, 455.
42. Honig, B., and Nicholls, A. (1995) *Science 268*, 1144.
43. Honig, B., and Yang, A.-S. (1995) *Adv. Protein Chem. 46*, 27.
44. McCammon, J. A. (1998) *Curr. Opin. Struct. Biol. 8*, 245.
45. Madura, J. D., Davis, M. E., Gilson, M. K., Wade, R. C., Luty, B. A., and McCammon, J. A. (1994) in *Reviews in computational chemistry* (Lipkowitz, K. W., and Boyd, D. B., Eds.) Vol. 4, pp 229−267, VCH Publishers, New York.
46. Simonson, T., and Brünger, A. T. (1994) *J. Phys. Chem. 98*, 4683.
47. Sitkoff, D., Sharp, K. A., and Honig, B. (1994) *J. Phys. Chem. 98*, 1978.
48. Horvath, D., van Belle, D., Lippens, G., and Wodak, S. J. (1996) *J. Chem. Phys. 104*, 6679.
49. Froloff, N. A., Windenmuth, A., and Honig, B. (1997) *Protein Sci. 6*, 1293.
50. Sharp, K. A. (1996) *Biophys. Chem. 61*, 37.
51. Zhang, T., and Koshland Jr., D. E. (1996) *Protein Sci. 5*, 348.
52. Yang, A.-S., Gunner, M. R., Sampogna, R., Sharp, K., and Honig, B. (1993) *Proteins: Struct., Funct., Genet. 15*, 252.
53. Antosiewicz, J., McCammon, J.-A., and Gilson, M. K. (1994) *J. Mol. Biol. 238*, 415.
54. Yang, A.-S., and Honig, B. (1995) *J. Mol. Biol. 252*, 351.
55. Yang, A.-S., and Honig, B. (1995) *J. Mol. Biol. 252*, 366.
56. Yang, A.-S., and Honig, B. (1996) *J. Mol. Biol. 259*, 873.
57. Hempel, X. (1995) *Biopolymers 36*, 283.
58. Smith, X. (1994) *Proteins: Struct., Funct., Genet. 18*, 119.
59. Ewing, T. J. A., and Lybrand, T. P. (1994) *J. Phys. Chem. 98*, 1748.
60. Helms, V., and McCammon, J.-A. (1997) *Protein Sci. 6*, 2336.
61. Tsingely, I., Grant, B. D., and Taylor, S. S. (1996) *Biopolymers 39*, 353.
62. Grant, B. D., Tsingely, I., Adams, J. A., and Taylor, S. S. (1996) *Protein Sci. 5*, 1316.
63. Gibson, R. M., and Ji-Buechler, Y., Taylor, S. S. (1997) *Protein Sci. 6*, 1825.
64. Friedman, R. A., and Honig, B. (1995) *Biophys. J. 69*, 1528.
65. Molecular Simulation Inc. (1992) Quanta version 4.0 parameter handbook, 200 Fifth Avenue, Waltham, MA 02154.
66. Frisch, M. J., Trucks, G. W., Schlegel, H. B., Gill, P. M. W., Johnson, B. G., Robb, M. A., Cheeseman, J. R., Keith, T., Petersson, G. A., Montgomery, J. A., Raghavachari, K., Al-Laham, M. A., Zakrzewski, V. G., Ortiz, J. V., Foresman, J. B., Cioslowski, J., Stefanov, B. B., Nanayakkara, A., Challacombe, M., Peng, C. Y., Ayala, P. Y., Chen, W., Wong, M. W., Andres, J. L., Replogle, E. S., Gomperts, R., Martin, R. L., Fox, D. J., Binkley, J. S., Defrees, D. J., Baker, J., Stewart, J. P., Head-Gordon, M., Gonzalez, C., and Pople, J. A. (1995) Gaussian 94, Revision E.1, Gaussian, Inc., Pittsburgh, PA.
67. Breneman, C. M., and Wilberg, K. B. (1990) *J. Comput. Chem. 11*, 361.
68. Helms, V., and Wade, R. C. (1997) *J. Comput. Chem. 18*, 449.
69. Brünger, A. T., and Karplus, M. (1988) *Proteins: Struct., Funct., Genet. 4*, 148.
70. Davis, M. E., Madura, J. D., Luty, B. A., and McCammon, J. A. (1991) *Comput. Phys. Commun. 62*, 187.
71. Madura, J. D., Briggs, J. M., Wade, R. C., Davis, M. E., Luty, B. A., Ilin, A., Antosiewicz, J., Gilson, M. K., Bagheri, B., Scott, L. R., and McCammon, J. A. (1995) *Comput. Phys. Commun. 91*, 57.
72. Lee, B., and Richards, F. M. (1971) *J. Mol. Biol. 55*, 379.
73. Gilson, M. K., Given, J. A., Bush, B. L., and McCammon, J. A. (1997) *Biophys. J. 72*, 1047.
74. Finkelstein, A. V., and Janin, J. (1989) *Protein Eng. 3*, 1.
75. Searle, M. S., Williams, D. H., and Gerhard, U. (1992) *J. Am. Chem. Soc. 114*, 10697.
76. Janin, J. (1995) *Proteins: Struct., Funct., Genet. 21*, 30.
77. Erickson, H. P. (1989) *J. Mol. Biol. 206*, 465.
78. Doig, A. J., and Sternberg, M. J. E. (1995) *Protein Sci. 4*, 2247.
79. Gerstein, M., Lesk, A. M., and Clothia, C. (1994) *Biochemistry 33*, 6739.

BI982064G